

## Coexistence of reentrant-spin-glass and ferromagnetic martensitic phases in the $\text{Mn}_2\text{Ni}_{1.6}\text{Sn}_{0.4}$ Heusler alloy

L. Ma, W. H. Wang, J. B. Lu, J. Q. Li, C. M. Zhen et al.

Citation: *Appl. Phys. Lett.* **99**, 182507 (2011); doi: 10.1063/1.3651767

View online: <http://dx.doi.org/10.1063/1.3651767>

View Table of Contents: <http://apl.aip.org/resource/1/APPLAB/v99/i18>

Published by the [American Institute of Physics](#).

---

### Related Articles

Surface spin glass and exchange bias effect in  $\text{Sm}_{0.5}\text{Ca}_{0.5}\text{MnO}_3$  manganites nano particles  
*AIP Advances* **1**, 032110 (2011)

Spin-glass magnetism of surface rich Au cluster film  
*Appl. Phys. Lett.* **99**, 022503 (2011)

Theory of magnetism with temporal disorder applied to magnetically doped ZnO  
*J. Appl. Phys.* **105**, 07E325 (2009)

Phase separation versus spin glass behavior in  $\text{La}_{0.85}\text{Sr}_{0.15}\text{CoO}_3$   
*J. Appl. Phys.* **105**, 07E320 (2009)

Magnetic ordering in the spinel compound  $\text{Li}[\text{Mn}_{2x}\text{Li}_x]\text{O}_4$  ( $x = 0, 0.04$ )  
*J. Appl. Phys.* **105**, 07D532 (2009)

---

### Additional information on *Appl. Phys. Lett.*

Journal Homepage: <http://apl.aip.org/>

Journal Information: [http://apl.aip.org/about/about\\_the\\_journal](http://apl.aip.org/about/about_the_journal)

Top downloads: [http://apl.aip.org/features/most\\_downloaded](http://apl.aip.org/features/most_downloaded)

Information for Authors: <http://apl.aip.org/authors>

### ADVERTISEMENT

**AIP**Advances

*Submit Now*

Explore AIP's new  
open-access journal

- Article-level metrics now available
- Join the conversation! Rate & comment on articles

# Coexistence of reentrant-spin-glass and ferromagnetic martensitic phases in the $\text{Mn}_2\text{Ni}_{1.6}\text{Sn}_{0.4}$ Heusler alloy

L. Ma,<sup>1,2</sup> W. H. Wang,<sup>2</sup> J. B. Lu,<sup>2</sup> J. Q. Li,<sup>2</sup> C. M. Zhen,<sup>1</sup> D. L. Hou,<sup>1</sup> and G. H. Wu<sup>2,a)</sup>

<sup>1</sup>Department of Physics, Hebei Advanced Thin Films Laboratory, Hebei Normal University, Shijiazhuang 050016, China

<sup>2</sup>Beijing National Laboratory for Condensed Matter Physics, Institute of Physics, Chinese Academy of Sciences, Beijing 100190, China

(Received 27 July 2011; accepted 15 September 2011; published online 2 November 2011)

A giant exchange bias field of up to 1170 Oe was observed in the  $\text{Mn}_2\text{Ni}_{1.6}\text{Sn}_{0.4}$  Heusler alloy. A reentrant spin glass phase and a ferromagnetic martensitic phase coexist below the blocking temperature as confirmed by dc magnetization and ac susceptibility measurements. Exchange bias in  $\text{Mn}_2\text{Ni}_{1.6}\text{Sn}_{0.4}$  is thought to originate from the interface exchange interaction between the reentrant spin glass phase and the ferromagnetic martensitic phase. X-ray diffraction and selected area electron diffraction results demonstrate that excess Mn atoms occupy Ni and Sn sites randomly. In this way, Mn-Mn clusters are formed and constitute the reentrant-spin-glass phase.

© 2011 American Institute of Physics. [doi:10.1063/1.3651767]

Recently, many Heusler alloys possessing the exchange bias (EB) property have been identified, including the Ni-Mn-X (X = Sb, Sn, and In) alloys.<sup>1–8</sup> Wang's group, in particular, has found that the EB field ( $H_E$ ) in  $\text{Mn}_2\text{Ni}_{1.6}\text{Sn}_{0.4}$  is as high as 910 Oe.<sup>9</sup> This is the largest value so far found in Ni-Mn-X Heusler alloys. The flurry of interest in the EB property stems from its application in magnetic read heads, spin valves, permanent magnets, and many other devices.<sup>10</sup> These important applications are based on the EB field created at the interface between ferromagnetic (FM) and antiferromagnetic (AFM) phases. Most investigators have thought that in Heusler alloys, the Mn atoms at regular sites constituted the FM phase and the excess Mn atoms at Ni or X (X = Sb, Sn, and In) sites acted as the AFM phase. The EB was then thought to originate from the AFM exchange interaction between the regular and excess Mn atoms.<sup>1–9</sup> However, the excess Mn atoms are coupled ferromagnetically, they are not suitable for use as the pinning phase (AFM phase), because the pinning phase should have higher magnetic anisotropy than the pinned phase (FM phase). This is why no EB phenomena have been observed in  $\text{Mn}_2\text{NiGa}$  Heusler alloy, although it has both regular and excess Mn atoms. In addition, considering that in this model both the regular and excess Mn atoms occupy the same lattice, that is to say, their relative positions are at the angstroms scale, whereas the FM and AFM phases should be separated by nanometers at least, it seems not appropriate to say that the regular Mn atoms serve as the FM phase and the excess Mn atoms act as the AFM phase. Thus, the physical mechanism of the EB in Heusler alloys is not clear at present. In this letter, we report the observation of a quite large EB field of up to 1170 Oe in the  $\text{Mn}_2\text{Ni}_{1.6}\text{Sn}_{0.4}$  alloy prepared by the deep cooling method and discuss in detail the physical mechanism of the EB.

$\text{Mn}_2\text{Ni}_{1.6}\text{Sn}_{0.4}$  was prepared by the arc melting method and annealed at 1073 K for 72 h, then quenched in liquid nitrogen. The crystal structure was characterized by x-ray

diffraction (XRD) and transmission electron microscopy—selected area electron diffraction (SAED, FEI Tecnai F20 operating at 200 kV). The magnetization measurements were performed in a physical property measurement system (PPMS-14, Quantum Design, Inc.) in the temperature range from 5 to 300 K.

Fig. 1 shows the magnetic hysteresis loops of the  $\text{Mn}_2\text{Ni}_{1.6}\text{Sn}_{0.4}$  sample measured in the field range of  $-2$  T to  $+2$  T after 0.05 T field cooling (FC) and zero field cooling (ZFC). For  $\text{Mn}_2\text{Ni}_{1.6}\text{Sn}_{0.4}$  after 0.05 T FC, the EB phenomenon is clearly observed with  $H_E = 1170$  Oe and  $H_C = 175$  Oe. The values are larger than those reported by Wang by  $\sim 200$  Oe and  $\sim 100$  Oe, respectively.<sup>9</sup> Both the composition and annealing temperature were the same as in Ref. 9, only the quench temperature is different, suggesting that the more rapid cooling may be the reason for the larger EB in our system.<sup>11</sup> On the other hand, double-shifted hysteresis is observed after ZFC. Similar behavior is often observed in some EB materials with inhomogeneous magnetic phases. In order to confirm this, ZFC and FC curves were measured as shown in the inset of Fig. 1. It can be seen that the ZFC and FC curves begin to split at 150 K.

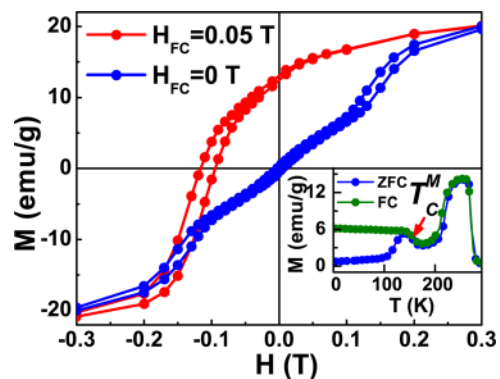


FIG. 1. (Color online) Magnetic hysteresis loops for a  $\text{Mn}_2\text{Ni}_{1.6}\text{Sn}_{0.4}$  sample measured at 5 K after 0.05 T FC and ZFC. The inset shows the ZFC and FC magnetizations as functions of temperature for the sample measured at a field of 0.01 T.

<sup>a)</sup> Author to whom correspondence should be addressed. Electronic mail: ghwu@aphy.iphy.ac.cn.

This suggests that different magnetic anisotropy phases exist in  $\text{Mn}_2\text{Ni}_{1.6}\text{Sn}_{0.4}$ . The Curie temperature of the martensitic phase ( $T_C^M$ ) was observed at about 160 K just below the martensitic transformation. Therefore, at least the FM martensitic phase should exist in  $\text{Mn}_2\text{Ni}_{1.6}\text{Sn}_{0.4}$  at low temperature.

Figure 2 shows the temperature behavior of the real ( $\chi'$ ) and imaginary ( $\chi''$ ) components of the susceptibility for  $\text{Mn}_2\text{Ni}_{1.6}\text{Sn}_{0.4}$  sample. It is remarkable that the shoulder at  $\sim 130$  K in the  $\chi'(T)$  curve shifts toward higher temperature with increasing frequency. This temperature at the shoulder is defined as the blocking temperature associated with the frequency  $T_f(\omega)$ , where  $\omega = 2\pi f$ . There is also a peak in the  $\chi''(T)$  curve which falls off suddenly near  $T_f(\omega)$ . This is an indication of a frustrated magnetic state. The value of  $\Delta T_f [T_f \Delta \log_{10} \omega]^{-1}$  can be used to describe the magnetic order of the system. This value typically lies between 0.005 and 0.08 for a spin glass (SG) and is  $\sim 0.1$  for noninteracting super paramagnetic materials.<sup>12</sup> For  $\text{Mn}_2\text{Ni}_{1.6}\text{Sn}_{0.4}$  sample, the value is 0.023. Therefore, the SG nature of  $\text{Mn}_2\text{Ni}_{1.6}\text{Sn}_{0.4}$  is strongly indicated by the AC measurements. It is interesting to observe that the other two shoulders at  $\sim 160$  K and  $\sim 170$  K also appear in the  $\chi'(T)$  curve but do not show any dependence on frequency. The former at  $\sim 160$  K also has a shoulder in the  $\chi''(T)$  curve and it should correspond to  $T_C^M$  according to the DC measurements shown in Fig. 1. On the other hand, the shoulder at  $\sim 170$  K does not have a signal in the  $\chi''(T)$  curve and likely corresponds to the Curie temperature of the SG phase ( $T_C^{\text{RSG}}$ ). Therefore, the SG phase in  $\text{Mn}_2\text{Ni}_{1.6}\text{Sn}_{0.4}$  is not a canonical spin glass but rather a reentrant spin glass (RSG).<sup>13</sup>

The discussion above may be summarized as follows. As the temperature is lowered from 180 K, the RSG phase in  $\text{Mn}_2\text{Ni}_{1.6}\text{Sn}_{0.4}$  first undergoes a transition at  $\sim 170$  K from a paramagnetic (PM) state to a FM state. Then, at  $\sim 160$  K, the martensitic phase in  $\text{Mn}_2\text{Ni}_{1.6}\text{Sn}_{0.4}$  also undergoes a transition from a PM state to a FM state. Finally, the RSG phase in  $\text{Mn}_2\text{Ni}_{1.6}\text{Sn}_{0.4}$  enters into a spin frustrated and frozen state at  $\sim 130$  K. This means that the short-range FM order RSG

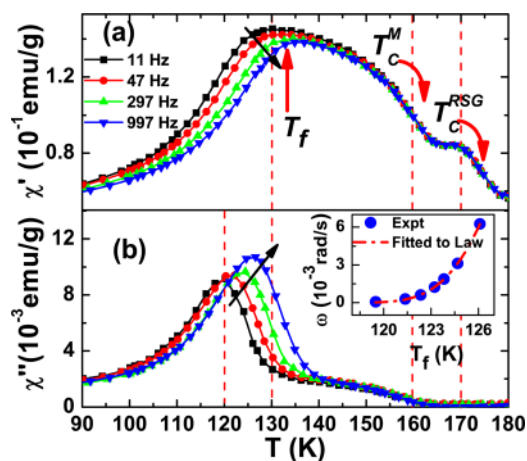


FIG. 2. (Color online) Temperature dependence of (a) real part and (b) imaginary part of the ac susceptibility measured at different frequencies with an ac magnetic field of 10 Oe, after ZFC to 5 K. The thin arrow indicates the direction of increasing  $f$  and the thick arrow represents the different characteristic temperatures. The inset shows the correlation between angular frequency ( $\omega$ ) and blocking temperature ( $T_f$ ).

phase and the long-range FM order martensitic phase are intrinsic separated phases in the  $\text{Mn}_2\text{Ni}_{1.6}\text{Sn}_{0.4}$  system.

In order to investigate the interaction among RSG clusters in  $\text{Mn}_2\text{Ni}_{1.6}\text{Sn}_{0.4}$  system, the Vogel-Fulcher law,  $\omega = \omega_0 \exp[-E_a/k_B(T_f - T_0)]$ , is adopted. In this expression,  $\omega$  is the measurement angular frequency,  $\omega_0$  is the characteristic frequency of the SG,  $E_a$  is the activation energy of the RSG,  $k_B$  is Boltzmann parameter,  $T_f$  is blocking temperature defined above, and  $T_0$  is the Vogel-Fulcher temperature describing the interaction among RSG clusters.<sup>14</sup> The best fit to the data is shown by the red line in the inset of Fig. 2. The fitted values of  $E_a/k_B$ ,  $\omega_0$ , and  $T_0$  are 75 K,  $2 \times 10^6$  rad/s, and 113 K, respectively. Note that the value of  $T_0$  is much larger than that for  $\text{Ni}_2\text{Mn}_{1.36}\text{Sn}_{0.64}$  (81.5 K).<sup>5</sup> This confirms that the exchange interaction among RSG clusters in  $\text{Mn}_2\text{Ni}_{1.6}\text{Sn}_{0.4}$  is stronger than that in  $\text{Ni}_2\text{Mn}_{1.36}\text{Sn}_{0.64}$ .

Fig. 3 compares the ZFC and FC hysteresis loops of  $\text{Mn}_2\text{Ni}_{1.6}\text{Sn}_{0.4}$  at 5 K. As is evident in inset (a), the ZFC hysteresis loop is symmetric and the FC hysteresis loop has a displacement along the field axis due to the EB. It is also interesting to observe that the ZFC curve is not easily saturated, as shown in inset (b). In fact, its saturation magnetization never matches that of the FC curve and its magnetization reversal is smooth, while the magnetization reversal of the FC curve suddenly speeds up in a negative field between  $-1.5$  T and  $-4$  T. The same kind of magnetic behavior is also observed between 1 T and 2 T. This indicates that some spin clusters of RSG could rotate with the applied field after 13 T FC. This fact can be interpreted in terms of a distribution of magnetically hard domain clusters. For the sample after ZFC, the clusters are assumed to stabilize in their own unidirectional anisotropy field of random orientation as shown in inset (c). In this case, the energy barrier between the clusters and the applied field which must be overcome during the magnetization process is different and varies continuously, so the magnetization reversal is smooth. On the other hand, for the sample after 13 T FC, the clusters would all stabilize in the same applied field orientation as shown in inset (d). In this case, the energy barrier is the same and lower than that of the ZFC sample, thus the sudden increase of magnetization noted above is observed during the magnetization reversal process.

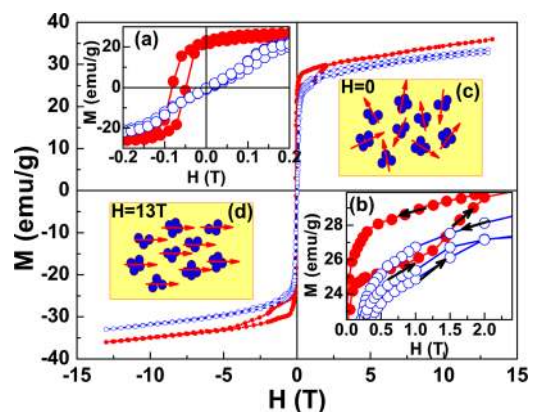


FIG. 3. (Color online) High field hysteresis loops for the  $\text{Mn}_2\text{Ni}_{1.6}\text{Sn}_{0.4}$  sample after 13 T FC (solid circles) and ZFC (open circles) to 5 K. The insets (a) and (b) are enlargements of the ZFC and FC  $MH$  curves and (c) and (d) are schematic drawings of the cluster spin configurations under ZFC and 13 T FC, respectively.



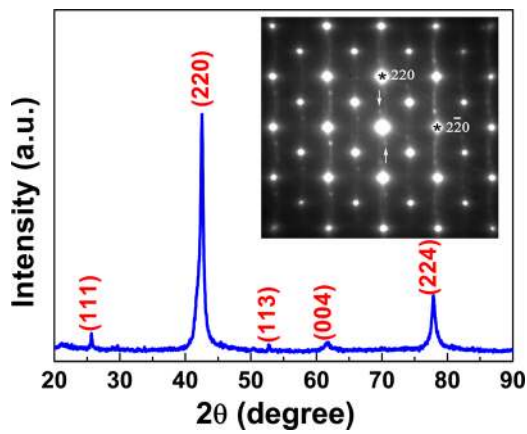


FIG. 4. (Color online) XRD patterns for  $\text{Mn}_2\text{Ni}_{1.6}\text{Sn}_{0.4}$  at room temperature. The inset shows SAED patterns of the sample along the [001] zone axis (arrows point to the diffuse reflections).

It was also noted that the value  $H_E = 650$  Oe (or  $H_C = 220$  Oe) of the sample after 13 T FC was smaller (or larger) than that of the sample after 0.05 T FC. Considering the EB system, two different opposite limiting cases can be predicted, depending on the strength of the pinning phase anisotropy. If the pinning phase anisotropy is large, one should observe only a shift of the hysteresis loop, while for small pinning phase anisotropies, the only observed effect should be a coercivity enhancement (without any loop shift).<sup>15</sup> As a result, we can conclude at least that the higher applied field destroys the macroscopic unidirectional anisotropy of the RSG phase.

Fig. 4 shows XRD patterns for  $\text{Mn}_2\text{Ni}_{1.6}\text{Sn}_{0.4}$ . The sample is a pure bcc structure with calculated lattice parameters of  $a = b = c = 6.010$  Å. Some order-dependent superlattice reflection peaks, such as (111) and (113), were also observed, but the (200) superlattice reflection peak was invisible. This indicates that the excess Mn atoms not only occupy Sn sites but also occupy Ni sites resulting in the enhancement of the (111) peak and the weakness of the (200) peak.<sup>16</sup> The inset of Fig. 4 shows the SAED pattern along the [001] zone axis in  $\text{Mn}_2\text{Ni}_{1.6}\text{Sn}_{0.4}$ . The main diffraction spots in this pattern can be well indexed as bcc structure, which is in agreement with the XRD results. Furthermore, some additional diffuse reflections can be clearly recognized. This demonstrates that visible local inhomogeneities exist in  $\text{Mn}_2\text{Ni}_{1.6}\text{Sn}_{0.4}$ , and are likely to be RSG regions. According to the investigation of Gigla *et al.*, the inhomogeneities may arise from atomic disorders.<sup>17</sup> Considering the excess Mn atoms and the deficiency of Ni and Sn atoms in  $\text{Mn}_2\text{Ni}_{1.6}\text{Sn}_{0.4}$ , the distribution of excess Mn atoms in the Ni and Sn sites is evidently random, so it is natural to assume that disordered Mn-Mn clusters are formed in the austenitic phase. The martensitic transition is a diffusionless transition. Thus, the Mn-Mn clusters should be maintained to low temperature. In this sense, the RSG phase is considered

as made up of disordered Mn-Mn clusters. It should be noted that the exchange interaction between the FM martensitic phase and the Mn-Mn clusters formed by Mn occupying Ni sites is much stronger than that between the FM martensitic phase and Mn-Mn clusters formed by Mn occupying Sn sites. This is because the Ni-Mn distance is shorter than that of Sn-Mn in Heusler alloys. Therefore, the high Mn concentration in  $\text{Mn}_2\text{Ni}_{1.6}\text{Sn}_{0.4}$  can dramatically increase the anisotropy of the RSG phase. This is the reason why the  $H_E$  in  $\text{Mn}_2\text{Ni}_{1.6}\text{Sn}_{0.4}$  is much larger than that in Ni-Mn-X.

In summary, we have observed giant exchange bias phenomenon ( $H_E = 1170$  Oe) in the  $\text{Mn}_2\text{Ni}_{1.6}\text{Sn}_{0.4}$  alloy using a deep cooling method. DC and AC magnetization measurements confirm that RSG and FM martensitic phases coexist below the blocking temperature ( $T_f = 117$  K). These two phases are responsible for the observed EB. The unidirectional magnetic anisotropy of the RSG phase in  $\text{Mn}_2\text{Ni}_{1.6}\text{Sn}_{0.4}$  is stronger than that in NiMnX alloys but lower than the AFM phase. XRD and SAED measurements indicate that the excess Mn atoms in  $\text{Mn}_2\text{Ni}_{1.6}\text{Sn}_{0.4}$  not only occupy Ni and Sn sites but also have a random occupation. Therefore, Mn-Mn clusters can be formed and compose the RSG phase.

This work is supported by National Natural Science Foundation of China (Grant Nos. 51021061, 51031004, and 51101049).

- <sup>1</sup>M. Khan, I. Dubenko, S. Stadler, and N. Ali, *Appl. Phys. Lett.* **91**, 072510 (2007).
- <sup>2</sup>M. Khan, I. Dubenko, S. Stadler, and N. Ali, *J. Appl. Phys.* **102**, 113914 (2007).
- <sup>3</sup>Z. Li, C. Jing, J. Chen, S. Yuan, S. Cao, and J. Zhang, *Appl. Phys. Lett.* **91**, 112505 (2007).
- <sup>4</sup>B. M. Wang, Y. Liu, L. Wang, S. L. Huang, Y. Zhao, Y. Yang, and H. Zhang, *J. Appl. Phys.* **104**, 043916 (2008).
- <sup>5</sup>S. Chatterjee, S. Giri, S. K. De, and S. Majumdar, *Phys. Rev. B* **79**, 092410 (2009).
- <sup>6</sup>C. Jing, J. Chen, Z. Li, Y. Qiao, B. Kang, S. Cao, and J. Zhang, *J. Alloys Compd.* **475**, 1 (2009).
- <sup>7</sup>A. K. Pathak, I. Dubenko, S. Stadler, and N. Ali, *IEEE Trans. Magn.* **45**, 3855 (2009).
- <sup>8</sup>A. K. Pathak, M. Khan, B. R. Gautam, S. Stadler, I. Dubenko, and N. Ali, *J. Magn. Magn. Mater.* **321**, 963 (2009).
- <sup>9</sup>H. C. Xuan, Q. Q. Cao, C. L. Zhang, S. C. Ma, S. Y. Chen, D. H. Wang, and Y. W. Du, *Appl. Phys. Lett.* **96**, 202502 (2010).
- <sup>10</sup>J. Nogués and I. K. Schuller, *J. Magn. Magn. Mater.* **192**, 203 (1999).
- <sup>11</sup>P. G. Debenedetti and F. H. Stillinger, *Nature* **410**, 259 (2001).
- <sup>12</sup>J. A. Mydosh, in *Spin Glasses: An Experimental Introduction* (Taylor & Francis, London, 1993), p. 68.
- <sup>13</sup>H. Maletta and W. Zinn, in *Handbook on the Physics and Chemistry of Rare Earths*, edited by K. A. Gschneidner, Jr. and L. Eyring (Elsevier, Amsterdam, 1989), Vol. 12, p. 314.
- <sup>14</sup>J. L. Tholence, *Solid State Commun.* **35**, 113 (1980).
- <sup>15</sup>J. Nogués, J. Sort, V. Langlais, V. Skumryev, S. Suriñach, J. S. Muñoz, and M. D. Baró, *Phys. Rep.* **422**(3), 65 (2005).
- <sup>16</sup>H. R. J. Wijn, in *Alloys and Compounds of d-Elements with Main Group Elements*, edited by P. J. Webster and K. R. A. Ziebeck (Springer, Berlin, 1988), Vol. 19/c.
- <sup>17</sup>M. Gigla, P. Szczeszczek, and H. Morawiec, *Mater. Sci. Eng., A* **438–440**, 1015 (2006).